12-1997

A Large Scintillation Detector for Nuclear Physics Experiments at Indiana University Cyclotron Facility

Apurva Pathak

A LARGE SCINTILLATION DETECTOR FOR NUCLEAR PHYSICS EXPERIMENTS AT INDIANA UNIVERSITY CYCLOTRON FACILITY

by

Apurva Pathak

A Thesis
Submitted to the
Faculty of The Graduate College
in partial fulfillment of the
requirements for the
Degree of Master of Arts
Department of Physics

Western Michigan University
Kalamazoo, Michigan
December 1997

ACKNOWLEDGEMENTS

I would like to begin by thanking Dr. Paul Pancella, my thesis advisor, for all the help and advice towards this thesis. Thanks are also due to members of the thesis committee, Dr. Gerald Hardie, Dr. Lisa Paulius and Dr. Alvin Rosenthal.

A word of thanks to Dr Robert Shamu for his concern towards this project. Beth and Lori in the Physics department office, thank you for your help from time to time. I would especially like to thank Robert Scherzer, for appreciating me as a teaching assistant and encouraging me. It was great working under your supervision.

Jeff Wroblewski and Michael Khazhinsky, my friends from the beginning of graduate school here at Western, who are now gainfully employed, thanks for your friendship and support over the years.

I owe a great debt of gratitude to my parents who have supported me whole heartedly in whatever I chose to do in life, even though it meant being thousands of miles away from them.

This would not be complete without thanking my wife Andra, for her constant support, encouragement and faith.

Apurva Pathak

A LARGE SCINTILLATION DETECTOR FOR NUCLEAR PHYSICS EXPERIMENTS AT INDIANA UNIVERSITY CYCLOTRON FACILITY

Apurva Pathak, M.A.

Western Michigan University, 1997

A new, large, scintillation detector, called the "K" detector has been designed and built for use in a series of nuclear physics experiments being performed at the Indiana University Cyclotron Facility (IUCF). This project describes the design, construction and testing of this scintillation detector. The K detector was designed to augment an existing detector stack at IUCF, and will serve to increase the energy range of previous studies of neutral pion production in proton-proton collisions near threshold. The test data for the current project came from a proton-proton scattering experiment, during which several runs were carried out between the bombarding proton energies of 200 MeV and 500 MeV. The scale factor, calculated to convert raw pulse heights into the energies deposited in the K detector by the forward scattered protons, exhibits angle dependence, indicating an angle or position dependence in the light collection efficiency of the K detector. In view of this angle dependence, a dimensionless angle dependent factor $F(\theta)$ was introduced and calculated, which produces a better agreement with the theoretical predictions for the energy lost by the forward scattered protons in the K detector. The angle dependence in the light collection efficiency of the K detector has been confirmed by the ongoing experiments at IUCF.

TABLE OF CONTENTS

LIST OF FIGURES

CHAPTER I

INTRODUCTION

The purpose of this project is to describe the design, construction, and testing of a new scintillation detector called the "K" detector.

The K detector was designed in late 1993 for use in a series of nuclear physics experiments being performed at the Indiana University Cyclotron Facility (IUCF). These experiments take place at an internal target station in the "Cooler", a storage ring and synchrotron for light ions.

The Indiana Cooler was proposed in 1980 shortly after Fermilab demonstrated that electron cooling does work as a mechanism for decreasing the phase volume of a stored ion beam. Phase space cooling makes it possible to pass the stored beam through a sufficiently thin internal target while maintaining a constant equilibrium emittance of the beam. Emittance corresponds to the area in phase space occupied by the particle beam. It was realized that nuclear physics experiments could benefit in many ways from this novel environment and that such a device could become an important new tool in nuclear physics. The Cooler consists of a six-sided magnet lattice of about 87 m circumference. The electron cooling system, region "C" in Figure 1, provides a co-moving electron beam of up to 2 A with a diameter of 2.5 cm over a

distance of 2.8 m. An rf cavity allows for the operation of the ring as a synchrotron. The synchrotron-cooler ring can provide protons with energies up to about 500 MeV. The maximum rigidity is 3.6 Tm, the transverse acceptances are 25 π mm mrad, and the momentum acceptance is 0.4%.

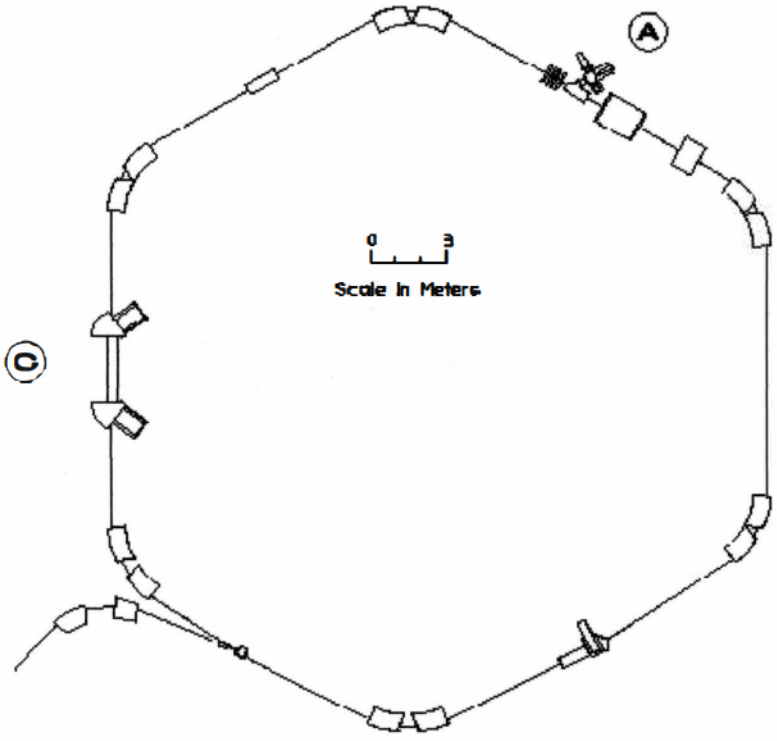

Figure 1. Layout of the Cooler Showing Regions "A" and "C".

The current series of experiments utilize the Cooler's capability of storing *polarized* proton beams, along with polarized target technology developed at the University of Wisconsin, Madison (Dezarn et al., 1995). This is interesting because the spin quantum number is known to play an important role in the strong nuclear force,

the force that holds nuclei together. In order to fully study the effects of spin in scattering experiments, it is necessary to polarize both the beam and the target particles. The IUCF Cooler combined with recent advances in polarized target technology have made such studies with a pure polarized target practical for the first time (Haeberli et al., 1997).

There are many advantages to the Cooler/internal target environment. Within the allowed range of beam energies, the beam energy can be varied and determined precisely. Small beam emittance allows small angle scattering to be observed. Use of thin targets facilitates measurement of final states and detection of the escaped low energy "recoil" particles. The absence of a beam-stop in the area generally results in a low-background environment.

The first Cooler experiment, CE01, performed in 1990, utilized many of the above mentioned advantages (Meyer et al., 1992). CE01 was a measurement of total cross section for $pp \rightarrow pp\pi^{\circ}$ in small energy steps close to threshold. This excitation function gives important information about the basic inelasticity in the nucleon-nucleon force. CE01 required the detection of coincident protons inside a forward cone of 20° half angle with good energy and angular resolution. The set up consisted of a multipurpose target box whose downstream end was a thin window to which the continuing beam pipe was joined by brazing. This window was followed by a sequence of scintillator and wire chamber planes. This arrangement of the scintillator detectors and wire chambers made the simultaneous detection of the two final state protons possible and also the measurement of their total energy up to 120 MeV, corresponding

to pion production at a beam energy of 325 MeV.

The "K" detector has been designed to augment the CE01 scintillator detector stack at IUCF. The primary use of this detector will be for the approved experiment CE44 ($pp \rightarrow pp\pi^{\circ}$ with polarized beam and polarized target) (Meyer, Horowitz, et al., 1992). The objective of CE44 is to measure the total cross section σ_{tot} and the spin-dependent total cross sections for $pp \rightarrow pp\pi^{\circ}$ between 300 MeV and 375 MeV bombarding energy. The extension to beam energies above 325 MeV requires the detection of higher energy final state protons, and thus increased thickness of the stopping detector, as described below.

Although the primary use of the K detector is intended for the experiment CE44 scheduled for 1997, the K detector was also used for another experiment, CE42, and that is where the test data for the current project came from (Przewoski et al., 1992). Both experiments are located in the "A" region of the Cooler (Figure 1).

CE42 measured the energy dependence of spin correlation parameters A_{xx}, A_{yy} and A_{xz} for pp elastic scattering at θ_{cm} up to 90°. The bombarding energy was varied in small steps in the energy range between 200 MeV and 500 MeV with particular emphasis on the region around 300 MeV, where inelastic channels open up.

Specific experiments lead to specific design requirements. In our case experiment CE44 guided the design requirements. The "K" detector, in combination with another scintillation detector, "E", will allow the range of energies to be extended upward for both experiments, CE42 and CE44. The primary purpose of this

new scintillation detector is to increase the upper energy limit of the present CE01 stack for doing a kinematically complete $pp \rightarrow pp\pi^{\circ}$ experiment with nearly full coverage of phase space. Where CE01 studied beam energies up to 325 MeV, the CE44 group proposes a maximum beam energy of 375 MeV. Basic $pp \rightarrow pp\pi^{\circ}$ kinematics at small scattering angle determine the required thickness for this detector. Corresponding to the maximum beam energy of 375 MeV for CE44, the maximum kinetic energy of the outgoing protons is 190 MeV. Our purpose is to stop the scattered protons in the scintillator detectors. The combined thickness of 0.2540 m of the E (0.1016 m) and the K (0.1524 m) detectors will enable us to do so. The K detector is segmented into four quadrants fitting the need to detect both protons simultaneously. Both E and K detectors are made of organic compounds mixed into a solid plastic. The phototubes are glued to the outside of the detector and not at the back in order to allow elastically scattered protons to pass through the detector and be detected in another layer of plastic scintillator.

The "K" detector is a thick plastic scintillation detector designed to measure the energy of nuclear radiation which passes through it. When a charged particle passes through matter it causes excitation and ionization of the molecules of the material. This ionization is the basis of all major instruments for the detection and measurement of such particles. When a particle impinges on certain materials known as phosphors, which possess the property of luminescence, part of the energy dissipated in molecular excitation and ionization is re-emitted as visible or ultra-violet photons. The observation and measurement of the light "flashes" or scintillations

produced in the phosphors by individual ionizing particles is the basis of the scintillation detector. The scintillations are converted into voltage pulses by photo-multiplier tubes and ultimately into a digital signal using amplifying and digitizing electronic circuits. The accuracy (or resolution) of the energy measurement requires the output signal to be proportional to the energy deposited by the original charged particle. The basic operation of a scintillation detector can be divided into five consecutive stages:

1. The absorption of incident radiation by the scintillator.
2. The scintillation process in which the energy dissipated in thescintillator is converted into luminescent emission of photons.
3. The transit of the emitted photons to the cathode of the photomultiplier.
4. The absorption of the photons at the cathode, the emission of photo-electrons and their collection at the first dynode.
5. The electron multiplication process.

These will be discussed in more detail in Chapter III.

A scintillator which is sufficiently thick allows total energy measurement of charged particles. Prior knowledge of target identity, beam identity and energy allows determination of the most likely identities of the final state particles. Combined with position sensitive detectors (MWPC's) this system allows momentum vector measurements in the final state. If enough momentum vectors are measured, the kinematics of each event are completely determined.

CHAPTER II

THE "K" DETECTOR

The "K" detector consists of the plastic scintillator, light guides, photo-multiplier tubes and the electronics for the amplification of the signal obtained from the photo-multiplier tubes. A brief description follows.

The detector is roughly a disk-shaped piece of scintillator 15 cm thick that completely surrounds the beam pipe (see Figure 2). The hole in the center of the scintillator allows the beam pipe to pass through. The scintillator material is a widely used plastic containing organic scintillation material (Bicron BC400). The outer diameter of the active area is about 85 cm, and is divided into four equal segments (see Figure 3). Each segment has three Plexiglas light guides glued to it, and each light guide has a phototube (Hamamatsu R 1250) mounted on it. The purpose of these light guides is to make the response of the phototubes less position dependent. To reduce light losses and to prevent outside light from leaking into the scintillator, each quadrant assembly is wrapped first in aluminum foil and then in thick black paper. These phototubes have flat circular photocathodes 12.7 cm in diameter. The phototubes are wrapped in "Mu-metal" (Advance Magnetics) to prevent the magnetic field present in the detector area from interfering with the initial amplification stages in the phototubes. Figure 4 shows the complete detector setup for CE42.

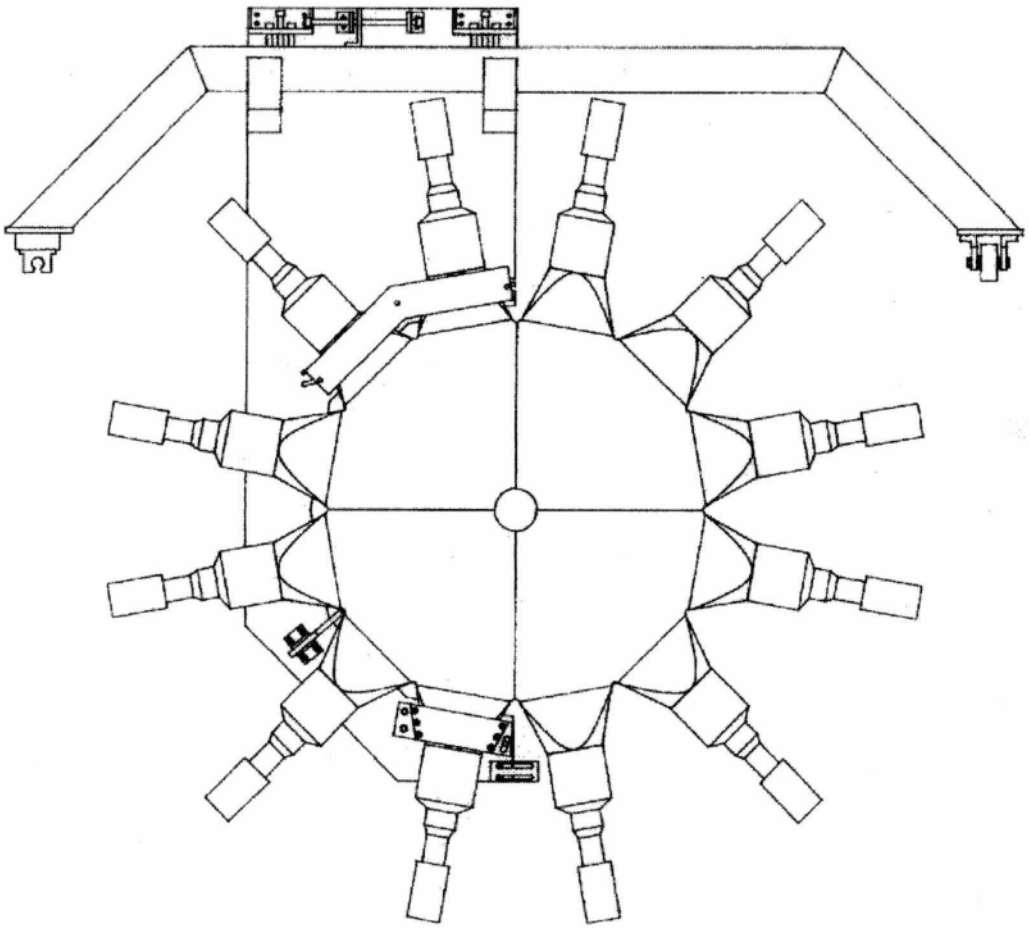

Figure 2. Front View of the K Detector. Part of the support structure has been removed for clarity.

Electronics

The high voltage channels (LeCroy) allow the voltage to be set remotely on the phototubes. They are the principal gain adjustment on the phototubes. The FERA ADCs (analog to digital converters) are peak-sensing ADCs, with 4096 channels precision. The logic modules are programmable and are used to set gains and offsets.

They have been adjusted to utilize all channels while accounting for overflows and underflows. Figure 5 shows the simplified electronics setup for one quadrant.

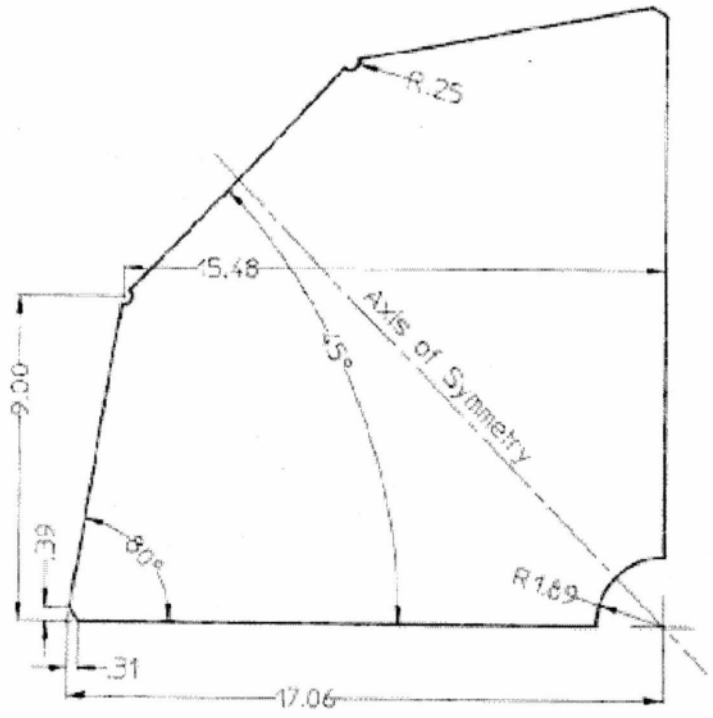

Figure 3. A Single Quadrant of the K Detector, Scintillating Plastic Only. Dimensions are in inches.

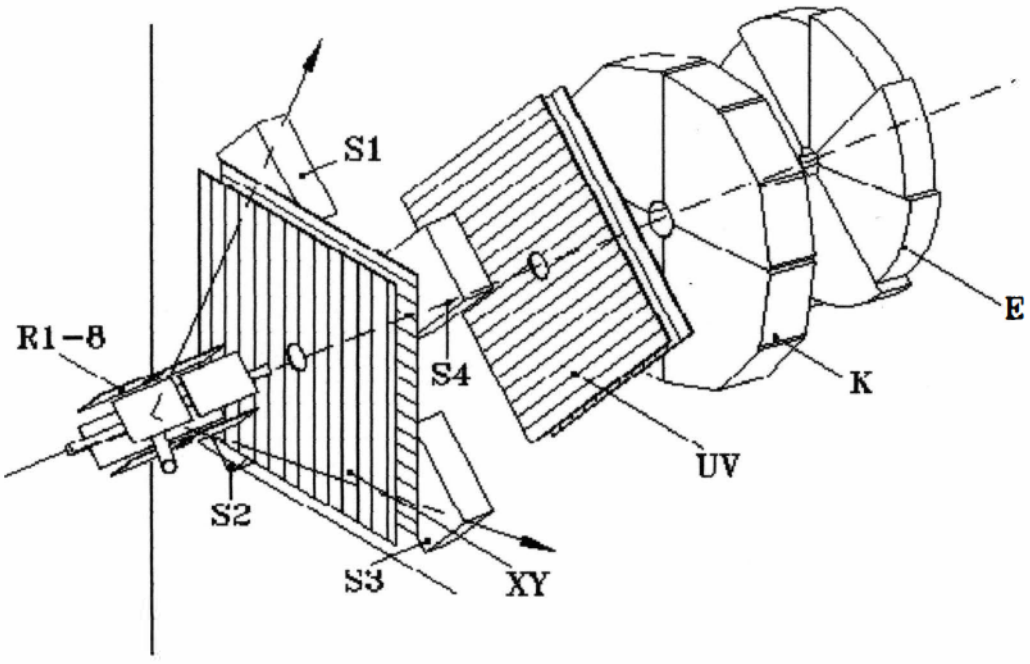

Figure 4. The Complete Detector Set up for CE42. The target cell is hidden among detectors R1-8 at left. Beam travels from left to right along dashed line. This setup is located in the "A" region of the Cooler (Figure 1).

Key to abbreviations

R1-R8 : R1-R8 are silicon strip detectors, each with a surface area of 4x8 centimeters.Each detector has 28 position sensitive strips each 2 mm wide. These detectors also give an energy signal. They are used to provide a coincidence with a forward going elastically scattered proton.

S1-S4 : S1-S4 are four plastic scintillators placed around the ϕ=45^0,135^0,225^0,315^0 points. Each detector covers scattering angles from 30 to 60 degrees in the lab. This set of detectors is used in conjunction with the XY wire chamber to measure pp elastic scattering at lab angles near 45^0.

XY,UV : XY and UV are wire chambers. The UV wire chamber is rotated 45 degrees relative to the XY chamber to resolve "left-right" ambiguity of wire hits in a single chamber. These two chambers are used to reconstruct the flight path of reaction protons so their scattering angles can be determined.

E,K : E and K are the segmented plastic scitillators.

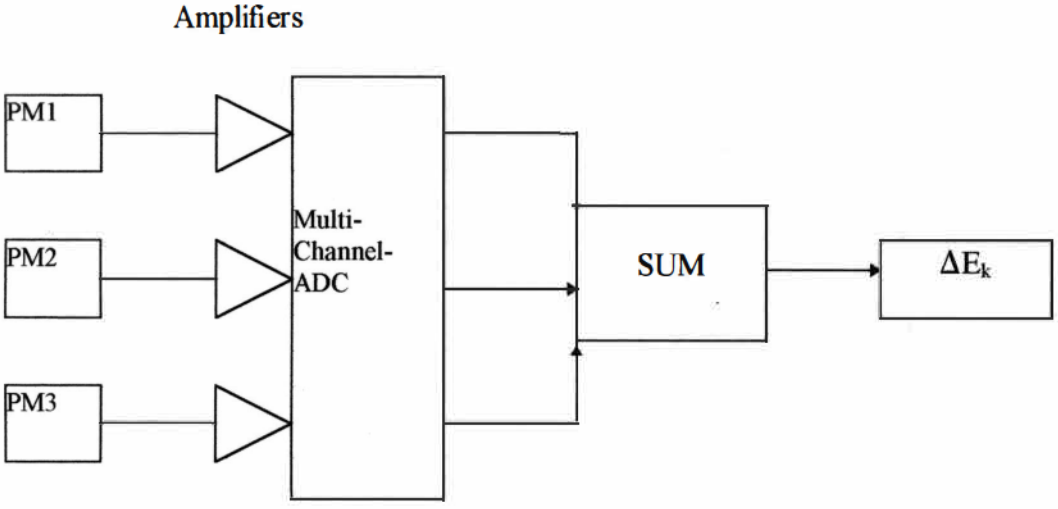

Figure 5. Basic Electronics for One Quadrant.

Key to abbreviations

PM1-PM3 : These are photomultiplier tubes 1 through 3, attached to one quadrant of the K detector.

ΔE_k : Sum of the pulse heights (energy lost in one quadrant of the K detector)

CHAPTER III

THEORY

Steps Between Charged Particle Entering the Scintillator and Digital Signal

Heavy charged particles in their passage through matter lose energy almost entirely through inelastic collisions with the bound electrons in the atoms of the stopping material. This process leads to a practically continuous attenuation of their energy as they progress through the stopping medium. The rate of energy loss decreases when the particle energy becomes low enough for it to capture electrons, but the slowing down will continue until the energy is reduced to the thermal energies of the atoms of the medium. The first part of the slowing down process, i.e., the slowing down during the time that the particle is charged, can be adequately treated from a theoretical point of view; the results of these calculations will be discussed below. However, when the charged particle is slow enough to capture electrons, i.e., below 1 MeV for alpha-particles and 0.1 MeV for protons, the theoretical problem becomes extremely difficult; it has not yet been solved. However, reasonably adequate experimental information is available and therefore, in what follows, the effect of such capture and loss of electrons on the ultimate range of a charged particle is taken empirically from the existing data.

Bethe's theoretical treatment of the energy loss is based upon the Born approximation applied to the collisions between the heavy particle and the atomic electrons (Segre et al., 1953). In this theory the differential cross section for a process in which the heavy particles transfer a given amount of energy to the atomic electrons is essentially given by the square of the matrix element of the Coulomb interaction between appropriate initial and final states. Plane waves are used for the wave functions of the incident and scattered heavy particle, the kinetic energies being E and E' < E, respectively. The condition of the atom is described initially by the unperturbed atomic wave function for the ground state and finally by the wave function for one of the excited final states. Multiplying the cross section for a given energy loss by the energy lost and summing over all possibilities gives the final expression for the average energy lost per centimeter of path.

Use of the Born approximation requires that the amplitude of the wave scattered by the field of the atomic electron shall be small compared to the amplitude of the undisturbed incident wave. As is well known, the criterion for this is that

$$\frac{ze^2}{\hbar v} << 1 \qquad (1)$$

where ze and v are the charge and velocity of the primary particle, respectively. This condition is well satisfied for large velocity and small charge of the incident particle. Equation (1) is also essentially the condition for the particle to have its full charge; when Eq. (1) is not fulfilled, the particle begins to capture electrons. The calculation of

the stopping power is made much simpler if the velocity of the particle not only fulfills Eq. (1) but is, in addition, large compared with the velocities of the electrons within the atom, i.e., if

$$E >> \frac{M}{m} E_{el} \tag{2}$$

where E is the energy of the incident particle, and E_{el} the ionizing potential of the electrons, and M and m the masses of the incident particle and the electron, respectively.

Under these conditions and for non-relativistic velocities the average energy loss per centimeter of path is

$$-\frac{dE}{dX} = \frac{4\pi e^4 z^2}{mv^2} NB \tag{3}$$

with

$$B = Z \log \frac{2mv^2}{I} \tag{4}$$

Here v is the velocity and ze the charge of the incident particle, N the number of atoms per cubic centimeter of the material, Z the nuclear charge, and I the average excitation potential of the atom. The term $-dE/dx$ is called the "stopping power" of the material traversed, and the dimensionless logarithm term B the "stopping number".

For relativistic velocities of the incident heavy particle it is shown by Bethe and Møller(Segre et al., 1953) that

$$B = Z\left\{\log\frac{2mv^2}{I} - \log(1-\beta^2) - \beta^2\right\} \qquad (5)$$

where $\beta = v/c$.

Scintillation in Organic Material

To understand the operation of a scintillator, we must consider the mechanisms by which energy can be absorbed in raising electrons to excited states (Krane, 1988). There are two basic types of detectors, those composed of organic materials and those composed of inorganic materials. The K detector is made of organic compounds mixed into a solid plastic.

In organic scintillators (which can be liquid or solid), the interactions between the molecules are relatively weak, and we can discuss their properties in terms of the discrete excited states of the molecules. There are two ways in which a molecule can absorb energy; the electrons can be excited to higher excited states, and the atoms in the molecule can vibrate against one another. Typical spacing between vibrational energy states is about 0.1 eV, while the electronic excitation energies are of the order of a few eV. The resulting structure may look something like that of Figure 6. The excited electrons are generally those not strongly involved in the bonding of the material. In aromatic hydrocarbons, such as those typified by the ring structure of benzene, three of the four valence electrons of carbon are in the hybridized orbitals

called σ orbitals; these are strongly localized between each carbon, its two carbon neighbors, and a single hydrogen. The fourth electron, which is in the so called π orbital, is not as well

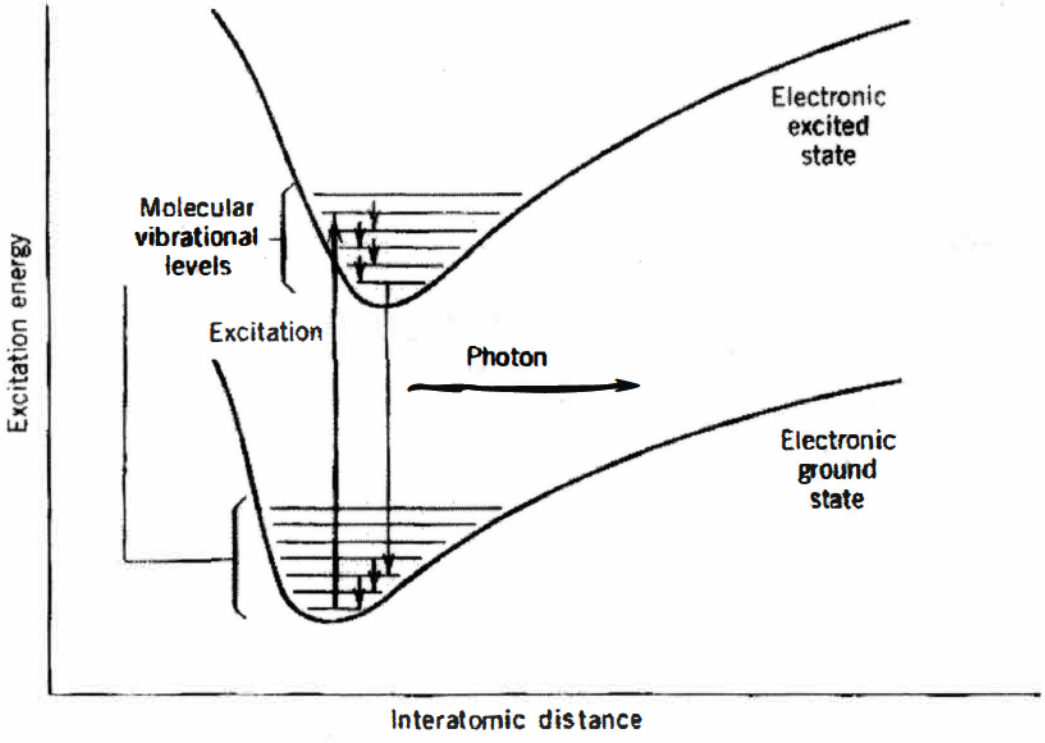

Figure 6. Electronic Structure in an Organic Scintillator.

localized and does not participate in the bonding process as strongly as the σ electrons. It is this π electron that is mostly responsible for the scintillation process.

The incoming radiation interacts with many molecules, losing a few eV at each interaction as it excites the molecule. Many possible vibrational states can be excited (and also many possible electronic excited states; for simplicity only the lowest

electronic excited state is shown). These decay quickly (~ 1 ps) to the lowest vibrational state of the electronic excited state, which then decays (in a time order of 10 ns) to one of the vibrational states of the electronic ground state.

Under normal circumstances, at room temperature all of the molecules of the scintillator are in the lowest vibrational state of the electronic ground state. The thermal energy kT at room temperature is 0.025 eV, and thus according to the Boltzmann population distribution $e^{-E/kT}$, it is unlikely to find any population of the vibrational states above the electronic ground state. Thus only one of the many emitted photon transitions has any probability to be absorbed. This represents an important property of a scintillator: *it must be transparent to its own radiation.*

The coupling of a scintillator to a photomultipler tube can be done in a variety of ways. Some detector-tube combinations are purchased as a sealed unit. Sometimes the photomultiplier geometry is very different from the scintillator geometry or it must be located far away from the scintillator (to eliminate the effects of magnetic fields, for instance). In this case a "light guide" is used; light guides can be cut to any size or shape out of any transparent material such as Lucite. The light guide should have nearly the same refractive index as the scintillator, and the joints made so as to reduce reflections as much as possible. Both the scintillator and the light guide must be wrapped with reflective material to improve the efficiency of light collection.

A schematic diagram of a PM tube is shown in Figure 7. A small number of electrons (smaller than the number of incident photons) is released at the photocathode, then multiplied and focused by a series of electrodes called dynodes.

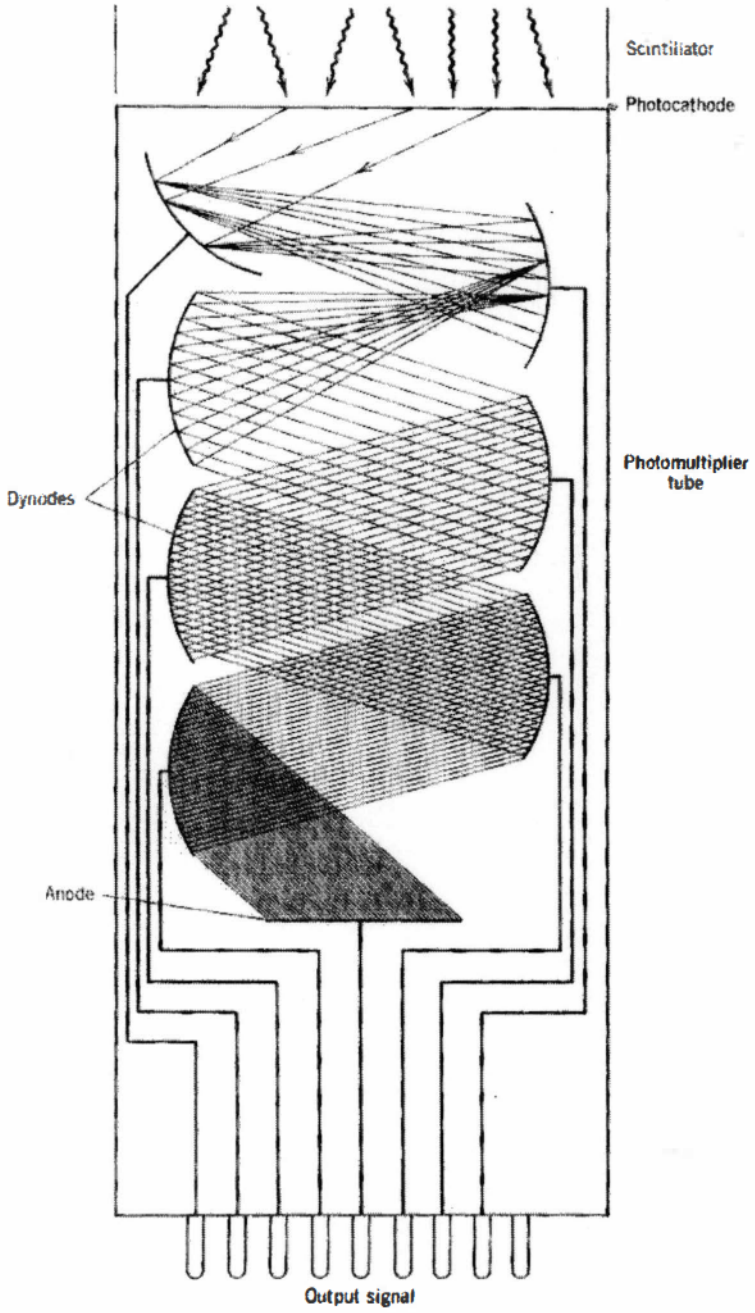

Figure 7. Schematic of a Photomultiplier Tube.

The dynodes are connected to a voltage chain produced by a high-voltage supply and a series of voltage dividers. The typical potential difference between adjacent dynodes is about 100 V and thus electrons strike the dynodes with about 100 eV of energy. The dynodes are constructed of materials with a high probability of secondary electron emission; it may take 2-3 eV to release an electron and thus a gain in the number of electrons of factors of 30-50 at each stage is possible. However, because the electrons are released in random directions in the material relatively few will actually be released at the surface, and a gain of 5 at each dynode is more typical. Even so, with a 10-dynode tube, the overall gain would be 5^{10} (about 10^7). For our purpose linearity is also an important characteristic . Linearity means that the amplitude of the eventual output pulse must be directly proportional to the original number of scintillation events and thus in turn to the energy deposited in the detector by the radiation. Because the gain of each dynode stage depends on the voltage difference, any change in the high voltage will cause a variation in the output pulse; thus it is often necessary to stabilize the high-voltage supply.

A wide variety of photomultiplier tubes is available; choices may be determined by such parameters as physical size, response of photocathode to different incident wavelengths, sensitivity of the photocathode, gain, noise level, and timing characteristics.

Therefore, the steps between a charged particle entering the scintillator detector and finally obtaining a digital signal can be summarized as follows:

1. The incident radiation enters the detector and suffers a large number of interactions which result in the raising of some atoms to excited states.

2. The excited states rapidly emit visible (or near visible) light; the material is said to fluoresce.

3. The light strikes a photosensitive surface, releasing at most one photoelectron per photon.

4. These secondary electrons are then multiplied, accelerated and formed into the output pulse in the photomultiplier tube and finally into digital signal by using amplifying and digitizing circuits (Birks, 1953).

CHAPTER IV

DATA FOR EVALUATION (CALIBRATION)

The test data for this project came from the experiment CE42, which is an elastic proton-proton scattering experiment. Although the "K" detector is primarily intended for experiment CE44, it was also used for CE42.

The goal of CE42 was to measure the energy dependence of the spin observables A_{xx}, A_{yy} and A_{xz} for pp elastic scattering at angles up to $\theta_{cm}= 90^{\circ}$. The bombarding energy was varied in small steps in the energy range between 100 MeV and 500 MeV with particular emphasis on the region around 300 MeV, where elastic channels open up. From the spin correlation parameters and the differential cross section the magnitude of the three amplitudes that completely describe the pp elastic scattering at $\theta_{cm}= 90^{\circ}$ was determined. The experiment made use of a polarized-hydrogen storage cell and a polarized, ramped beam. Complete angular distributions were obtained simultaneously, making use of the forward array (figure 4, chapter 2).

Four groups of plastic scintillators were placed at $\phi= 45^{\circ}$, 135°, 225° and 315° to allow coincident detection of both outgoing protons in the vicinity of $\theta_{cm}= 90^{\circ}$. Each group consists of 4 detectors S1-4 (Figure 4, Chapter II) allowing a measurement of the angular distributions around 90°. For the forward angles, the

forward array was used simultaneously. In this case, the forward scattered proton is detected by the forward array while the recoil proton is detected with Si-strip detectors alongside the target cell.

Unlike CE44, the forward scattered protons are not being stopped in the detector stack. However, the Bethe-Bloch equation still applies and was applied for this analysis. To aid in calibration, measurements are made at two different beam energies during every run. At the beginning of each run a beam at energy 197 MeV is injected into the Cooler ring, which is later ramped to the desired beam energy for that particular run.

Figure 8 is an example raw spectrum, a two-dimensional histogram with the number of counts indicated by the size of the boxes. The pulse heights (x axis) from the K detector, for a given event should be proportional to the energy lost by the forward scattered protons at different lab angles (y axis) for the pp elastic scattering experiment. During the course of the CE42 experiment several runs were carried out between the bombarding proton energies of 200 MeV and 500 MeV. The trigger for an event to appear on the raw spectrum is a coincidence between the "K" detector and one of the Si-strip detectors alongside the target cell (Figure 4). According to the conservation of energy and momentum in a pp elastic scattering, as the forward scattered proton is scattered at larger lab angles, the less energetic it becomes, and thus deposits *more* energy in the "K" detector, in keeping with the Bethe-Bloch equation. This results in higher pulse heights in the raw spectrum. The two groups of counts in figure 8 correspond to two different bombarding proton energies, 450 MeV

and 197 MeV. The higher group of pulse heights are due to the lower bombarding energy, 197 MeV, also in accordance with the Bethe-Bloch equation.

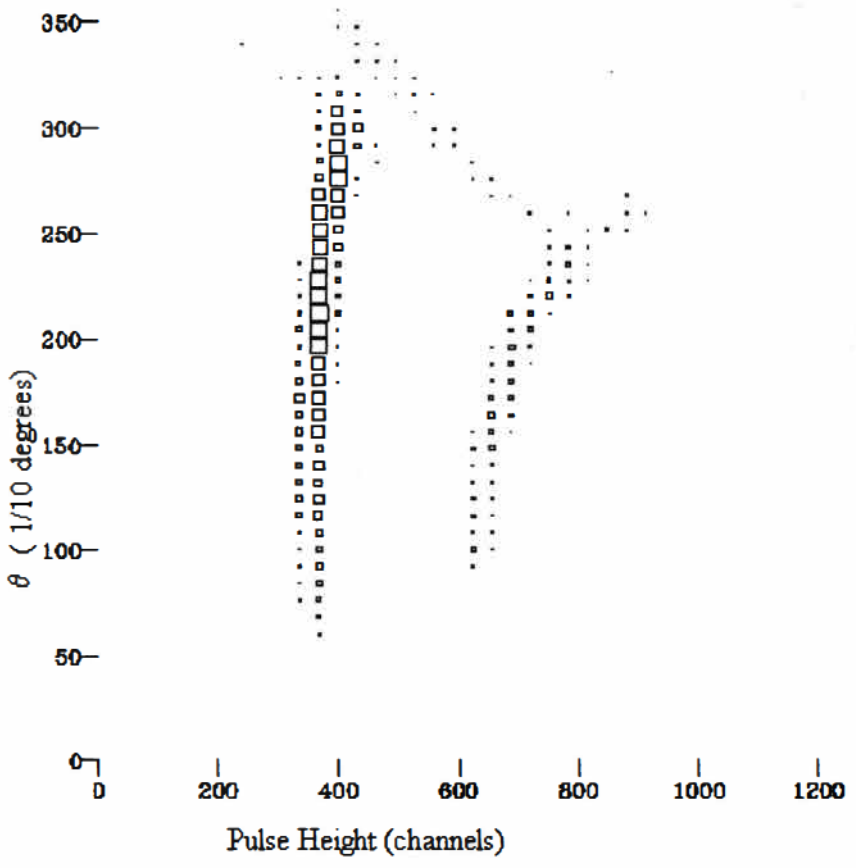

Figure 8. Example Raw Spectrum.

The proton beam is well centered with the detector stack which has a hole in the center for the beam to pass through. There is a small cosine effect in the thickness of the "K" detector for up to θ_{lab}= 28°. Upwards of θ_{lab}= 28° the corner of the detector comes into play and the thickness drops sharply to zero. Figure 9 depicts the situation.

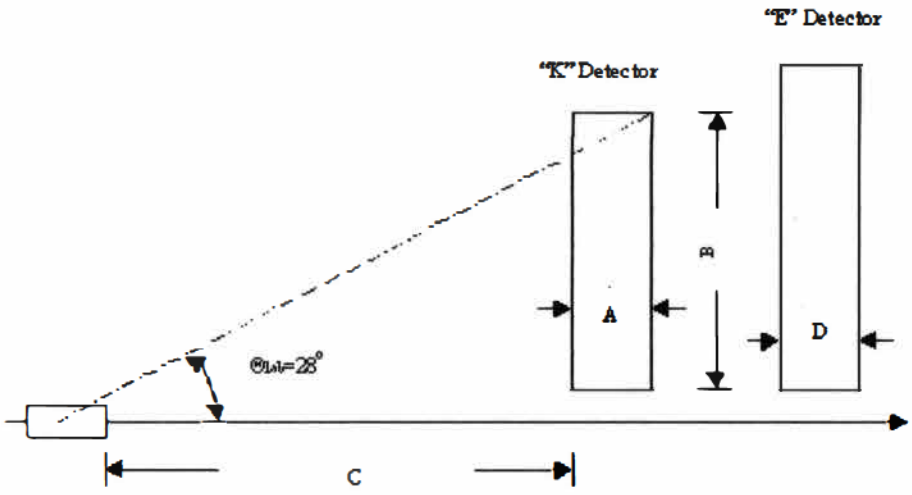

Figure 9. Cutaway Side View Half of "K" and "E" Detector. Target chamber and other details have been suppressed for clarity. Figure has not been drawn to scale.

Key to dimensions in Figure 9.

A= Thickness of the "K" detector ~ 152 mm
B= Radius of the "K" detector ~ 432 mm
C= Distance from the target cell to the "K" detector ~ 922 mm
D= Thickness of the "E" detector ~ 102 mm

A similar raw spectrum was used to find the relationship between pulse height and energy deposited in the K detector. The data were separated by taking the centroids of the pulse heights for each angle bin on the Y axis. The energy lost in the K detector was calculated for each angle bin, taking the forward scattered protons' path through increasing thickness of the K detector into account. All forward scattered protons punch through the K detector. An average scale factor(0.1943 MeV/channel) and an average offset (-32.79 MeV) were found over all angle bins using two different bombarding proton energies (197 MeV, 400 MeV). Using this average scale factor 'r'

and offset, the pulse heights for a third bombarding energy (310 MeV) were scaled to obtain the energy lost in the K detector.

$$\Delta E = \text{offset} + r(\text{Pulse Height}) \quad (6)$$

This measured energy loss ΔE was compared with the theoretical energy loss, $\Delta E_{theoretical}$, in the K detector as predicted by the Bethe-Bloch equation. The scale factor 'r' was used to convert the pulse heights from the raw spectrum to the energy deposited in the K detector. Figure 10 shows a bar plot for $\Delta E_{theoretical}-\Delta E$ versus θ_{lab} for the bombarding proton energy of 310 MeV. Once again, $\Delta E_{theoretical}$ takes into account the kinematics of the pp scattering and the increasing apparent thickness of the detector at larger scattering angles.

Figure 10 suggests an angle or position dependence in the light collection efficiency of the K detector. In view of this behavior, an angle dependent factor $F(\theta)$ was introduced such that, the measured energy loss ΔE was changed to

$$\Delta E = F(\theta)[\text{offset} + r(\text{Pulse Height})] \quad (7)$$

where $F(\theta)$ is a dimensionless factor introduced to account for the angle dependence in the light collection efficiency of the K detector. The scale factor 'r' is the same as above. $F(\theta)$ was calculated keeping the scale factor and offset fixed. Using $F(\theta)$, the pulse heights for the third energy (310 MeV) were calculated again, producing a better agreement with the energy loss predicted by the Bethe-Bloch equation. Figure 11

shows the bar plot of $\Delta E_{theoretical}$-ΔE versus θ_{lab}, taking the new angle dependent factor $F(\theta)$ into account. Figurel 2 shows a plot of $F(\theta)$ versus Lab angle θ.

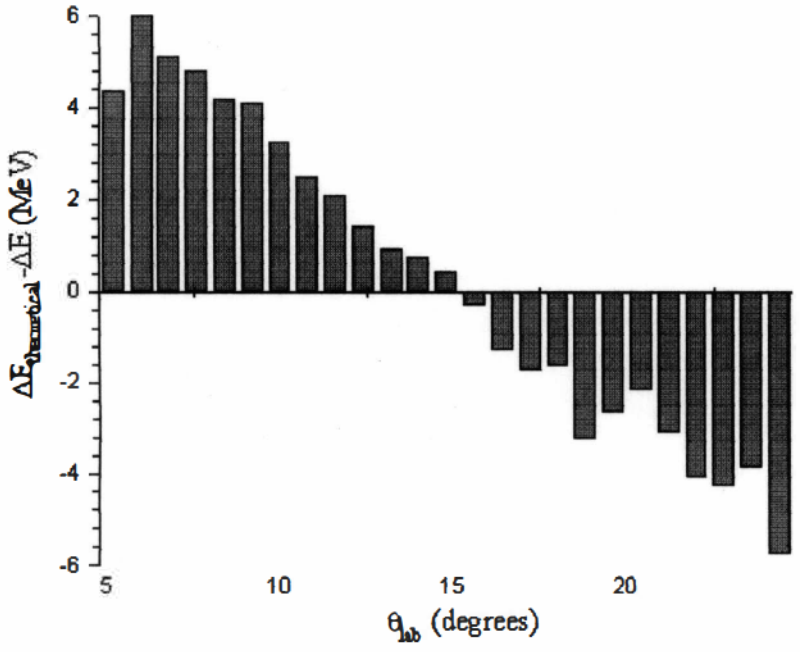

Figure 10. Bar Plot of $\Delta E_{theoretical}$-ΔE Versus θ_{lab}.

Conclusions

Figure 10 shows that there is an angle dependence in the pulse heights from the K detector which is not explained by kinematics or the geometry of the detector. The data indicate that there is more efficient light collection for particles scattered at lower angles or farther away from the phototubes (closer to the center of the detector). This is in contrast to what we instinctively expected, originally. The signal

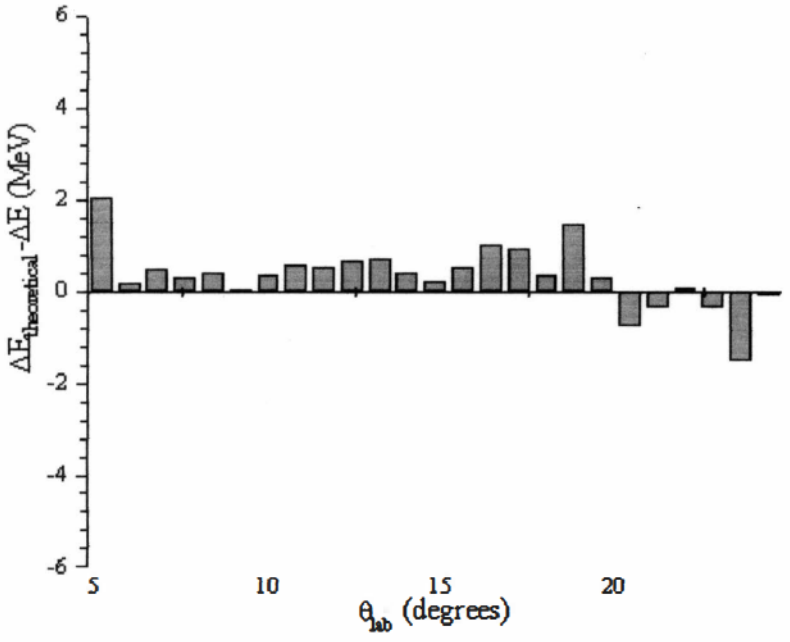

Figure 11. Bar Plot After Taking F(θ) Into Account.

from each quadrant of the K detector is a sum of the signals from all three PM tubes in that quadrant, as shown in the schematic of the basic electronics in Figure 5. As the scattered particle gets closer to one of the phototubes, the signal obtained by the other two phototubes due to the same scattered particle in the same detector quadrant appears to be deteriorating. It is probable that a better sum of the three PM tubes is being obtained for particles scattered at lower angles (or farther from the phototubes). It seems likely that at higher angles (or closer to the phototubes) all the three PMtubes are not contributing equally due to the scattered particle being closer to one tube as compared to the others.

This is not the final word in the evaluation and calibration of the "K" detector. More work is needed, especially for the CE44 experiment, using data with lower beam energies, for which the "K" is to function as a stopping detector.

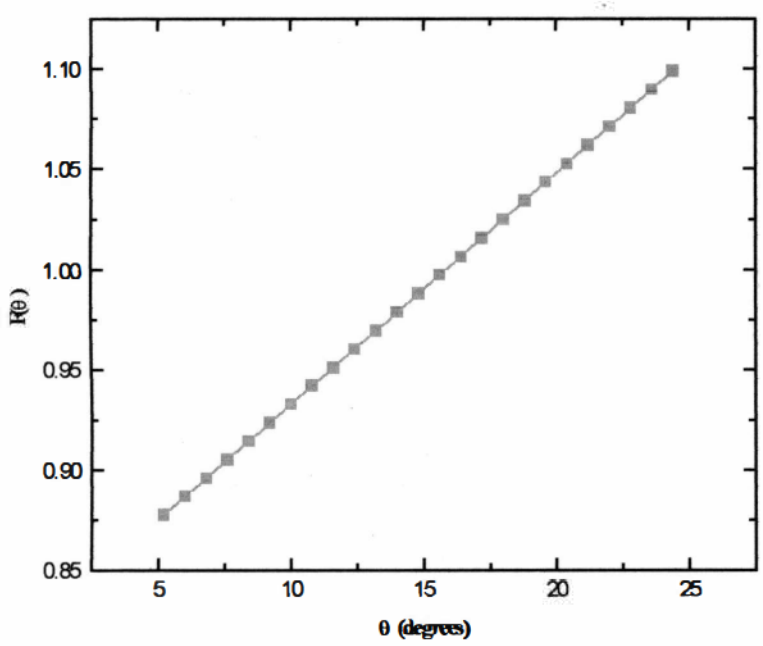

Figure 12. F(θ) Versus θ.

BIBLIOGRAPHY

Birks, J.B. (1953). *Scintillation Counters*. New York: McGraw Hill Book Co., Inc

Dezarn, W.A., Doskow, J., Hardie, J.G., Meyer, H.O., Pollock, R.E., Przewoski, B. von, Rinckel, T., Sperisen, F., Haeberli, W., Lorentz, B., Rathmann, F., Ross, M.A., Wise, T. and Pancella, P.V. (1995). Polarization Internal Gas Target for Hydrogen and Deuterium at the IUCF Cooler Ring. Nuclear Instruments and Methods in Physics Research, A362, 36.

"Glossary of Accelerator Terms". Available at: <http://adwww.fnal.gov/www/operations/accgloss/gloss.html>

Haeberli, W., Lorentz, B., Rathmann, F., Ross, M.A., Wise, T., Dezarn, W.A., Doskow, J., Hardie, J.G., Meyer, H.O., Pollock, R.E., Przewoski, B.von, Rinckel, T., Sperisen, F. and Pancella, P.V. (1997). Physical Review, C55, 597.

"IUCF Home Page". Available at: <http://www.iucf.edu>

Krane, K.S.(1988). *Introductory Nuclear Physics*. John Wiley & Sons.

Meyer, H.O.(1989). Preparations for research with the Indiana Cooler. Nuclear Instruments and Methods in Physics Research, B43, 383-389.

Meyer, H.O.(1992). $pp \rightarrow pp\pi^o$ with polarized beam and polarized target. Research Proposal to the Indiana University Cyclotron Facility.

Meyer, H.O., Horowitz, C., Nann, H., Pancella, P.V., Pate, S.F., Pollock, R.E., Przewoski, B. von, Rinckel, T., Ross, M.A. and Sperisen F. (1992). Total Cross Section for $pp \rightarrow p+p+\pi^o$ close to threshold. Nuclear Physics A, A539, 633-661.

Pancella, P.V. (1994). "E2" Design Report.

Pancella, P.V., Pathak, A., Komisarcik, K., Doskow, J and Przewoski, B. von. (1994). Increased stopping power for the "CE01" detector stack. Indiana University Cyclotron Facility Scientific and Technical Report.

Przewoski, B. von.(1992). Measurement of pp spin correlation parameters at θ_{cm}=90° in the energy range between 100 and 500 MeV. Research Proposal to the Indiana University Cyclotron Facility.

Segre, E., Staub H., Bethe, H., Ashkin, J., Ramsey, N.F., Bambridge, K.T. (1953). *Experimental Nuclear Physics*. John Wiley & Sons. New York, London.